Available online at www.sciencedirect.com
ScienceDirect
Journal of Sound and Vibration 304 (2007) 1–17
JOURNAL OF SOUND AND VIBRATION
www.elsevier.com/locate/jsvi

Viscous oscillations in a circular cylindrical tank with elastic surface cover

H.F. Bauer[a], M. Chiba[b,*]

[a]*Institut für Raumfahrttechnik, Universität der Bundeswehr München, 85577 Neubiberg, Germany*
[b]*Department of Aerospace Engineering, Graduate School of Engineering, Osaka Prefecture University, 1-1 Gakuen-cho, Naka-ku, Sakai 599-8531, Japan*

Received 8 November 2004; received in revised form 26 July 2006; accepted 15 January 2007

Abstract

In order to shift the frequencies of a liquid with a free surface away from dangerous system frequencies, the surface of the liquid may be covered with a flexible membrane or a thin elastic plate. The magnitude of such a frequency shift depends on the parameters of the liquid and those of the structural system and should be known for the design of an aerospace vehicle. For that reason, we treat a rigid circular cylindrical large aspect ratio container filled with incompressible and viscous liquid, being covered by an elastic structure. The coupled frequencies and the decay magnitudes are determined for the lower vibration modes. The fact that we deal with a large aspect ratio tank, where the liquid close to the bottom of the container exhibits only small velocities, suggests that the adhesive bottom conditions may be deleted, while those at the side wall of the container are mainly contributing to the damping and are for that reason considered in the analysis. We determine the complex frequencies of the hydroelastic system. The results show that the coupled frequencies increase with increasing liquid height ratio and reach soon a nearly constant value, which is being reached much earlier for higher modes. The decay magnitude also reaches quickly a constant value. Higher modes are damped out fast. In addition, it was found that the coupled oscillation frequencies are always larger than those of the frictionless liquid, and that the difference between them decrease considerably with increasing mode numbers.

1. Introduction

In modern technology, there is a predominant trend for thin and light structures, leading to high flexibility of such systems. This is the case for large-capacity liquid containers, propellant storage tanks or for containers in airplanes, missiles, space vehicles, satellites or space stations. In aerospace vehicles, we find often strong interactions of propellants with the elastic structure and mainly with the control system. Especially containers of large diameters exhibit low natural frequencies proportional to the reciprocal square root of the diameter, and more dangerously, very large sloshing masses, being proportional to the third power of the diameter. These interactions usually endanger the integrity of the system and may finally destroy the success of the mission. In such cases, the shifting of those frequencies which lead to instability, is usually the only way to

*Corresponding author. Tel./fax: +81 72 254 9235.
E-mail address: chiba@aero.osakafu-u.ac.jp (M. Chiba).

0022-460X/$ - see front matter © 2007 Elsevier Ltd. All rights reserved.
doi:10.1016/j.jsv.2007.01.045

Nomenclature

A, B, C, D	coefficients in Eq. (15)
A_{mn}, B_{mn}, C_{mn}, D_{mn}	coefficients in Eqs. (17)–(20)
A^*_{mn}	$\equiv A_{mn}a^2/v$
a	radius of tank
$\bar{D}$	flexural rigidity of plate
E	Young's modulus of plate
g	gravitational acceleration $g^* :\equiv ga^3/v^2$
h	liquid height
I_m	modified Bessel function of order m
i	imaginary unit
J_m	Bessel function of the first kind of order m
k	constant in Eqs. (7)–(10) $K :\equiv ka$
$K_{mn}(S)$	roots of transcendental Eq. (23)
$\bar{K}$	distributed stiffness of torsional spring (moment/unit length) for elastically supported boundary condition
M	number of division
m	number of nodal diameter
M_r	moment
n	number of nodal circle
p	liquid pressure
p_o	static liquid pressure
r, φ, z	coordinate system
S	$\equiv sa^2/v = \delta \pm i\omega$
s	characteristic index $\equiv \bar{\sigma} \pm i\bar{\omega}$
T	tension of membrane
T^*	$\equiv Ta/\rho v^2$ membrane tension parameter
t	time
u, v, w	velocity components of liquid
V_r	shear force
β^2	$\equiv a^2(\bar{\mu}s^2 + \rho g)/T = (\mu^* S^2 + g^*)/T^*$
β_{mn}, γ_{mn}	parameters in Eqs. (24) and (25)
$\bar{\delta}$	plate thickness
σ	tension of liquid surface
$\bar{\eta}$	dynamic viscosity of liquid
$\bar{\mu}$	mass/unit area of membrane or plate
μ^*	$\equiv \bar{\mu}/\rho a$
ν	$\equiv \bar{\eta}/\rho$
$\bar{\nu}$	Poisson's ratio of plate
ξ, η, $\bar{\zeta}$	displacement components of membrane or plate
$\bar{\zeta}_{mn1}$, $\bar{\zeta}_{mn2}$	coefficients in Eq. (29)
ρ	density of liquid
ϕ, ψ	functions defined by Eq. (5a)
ω	Im $S = \bar{\omega}a^2/v$
δ	Re $S = \bar{\sigma}a^2/v$

remedy such disturbing and dangerous problems. Such a procedure may, in some cases, be achieved effectively by covering the free liquid surface with a flexible structural member, such as a membrane or a thin elastic plate of various possible boundary conditions. With such a covering the coupled structural member's frequencies are shifted away from those of the dangerous one of the original system. It is, of course, mandatory to know the magnitude of these hydroelastic frequencies and assure the designer that they are separated to a great extent from and above the control frequency [1,2]. In Ref. [2] a "sliding-friction"-edge condition has been considered, treating a non-viscous liquid with a sloshing free liquid surface in such a way, that the edge condition could be changed with the "sliding-friction" coefficient. The limit case $\kappa \to \infty$ represents the edge-surface line at the container wall as a slipping line, while the magnitude of κ being zero describes this line as an anchored edge, i.e. fixed or stuck edge line. This yields larger natural frequencies for the sloshing modes and would be more adequate to the comparison of a sloshing liquid to that of the liquid-membrane motion at hand, since the membrane edge is also fixed.

In recent years, some of the early research activities in the hydroelastic area, where a lot of experiments and analyses [3–24] have been performed for cylindrical containers partially filled with frictionless liquid, emphasized the importance of such hydroelastic investigations. Some of them treated the interaction with the elastic cylinder wall [3–7,11–17,19], while others investigated the effect of an elastic tank bottom on the sloshing of the frictionless liquid. Similar treatments have also been performed on rectangular container [25–27], and for a cylindrical container with partial cover [28]. If the free liquid surface is completely covered by an elastic structure, the natural frequencies of the liquid-structure system shall yield the desired increase of the magnitude of the frequencies [18,25]. This increase depends mainly upon the tension or stiffness of the elastic coverage. In all these investigations, the liquid has been assumed to be incompressible and frictionless. Recently, the coupled frequencies of a liquid in a circular cylindrical container with an elastic cover and filled with non-viscous liquid has been determined by Bauer [25]. For a viscous liquid no results have been known until recently. Bauer and Chiba [29] have determined the damped coupled frequencies for a viscous liquid in a

tank of small liquid height ratio, i.e. a shallow container. In this treatment, adhesive conditions were satisfied at the container bottom and the elastic cover, while at the small side wall area only the normal velocity condition has been observed. This seems to be justified for shallow containers, in which nearly all the liquid participates in sloshing. The analytical treatment yields approximate complex frequencies, of which the real parts describe the damping decay, while the imaginary parts represent the oscillation frequencies. The procedure is based on the fact that in a shallow tank, say at least $h/a<0.5$, the friction at the side wall may be neglected in comparison with that on the combined magnitude of that of the tank bottom and top. The top and bottom area of the liquid is $2\pi a^2$, while the side wall area is $2\pi ah$. The smaller h, the smaller the contribution of the side wall to the damping—justifying the neglection of the adhesive conditions there—since the area ratio is h/a. This is only a rough estimate. In Ref. [29], we have investigated the liquid-structure behavior only for values $h/a<0.5$. This was performed in order to find the motion behavior in that region, resulting in—as for a viscous liquid with a free liquid surface—a range h/a for which only aperiodic motion is possible, indicating vanishing oscillation frequency and very large decay magnitude. For very small aspect ratio h/a, the damping contribution from the membrane and the container bottom is very large, thus reducing the oscillation frequency of the coupled system to very small values and increasing the decay magnitude of the membrane-liquid system to large values. At a certain small h/a-value the oscillation frequency even vanishes and the system exhibits only aperiodic motion. With increasing aspect ratio h/a, the influence of the container bottom decreases and diminishes as the ''sloshing plug''-height is reached. With further growth of the liquid-height ratio h/a, we shall approach the oscillation frequency of the large aspect ratio tank. Both solutions, i.e. the one of [29] and that presented here, are approximations to an exact solution which is not yet available. For that reason—and especially for the assumed analytical structure of these two cases the results cannot coincide and cannot exhibit at a certain h/a-value complete agreement. This was also detected in Refs. [30,31] where the oscillation frequencies of both cases differ from each other. The decay magnitude of the case with wall friction is in the oscillatory range always larger than that of the case where the friction of the tank bottom and an anchored free surface-edge line was considered. We must emphasize that for these reasons we cannot expect a complete agreement in the transition zone from shallow to large aspect ratio containers.

It was found that viscosity decreases the oscillation frequencies in comparison to the coupled hydroelastic frequencies of the frictionless liquid and that a new phenomenon appears exhibiting for certain small liquid heights h/a only aperiodic motion. With increasing angular and radial mode numbers, these aperiodic ranges decrease. In addition, it was found that higher modes exhibit larger damping. An increase of the membrane tension decreases the aperiodic region, while an increase in the mass of the membrane increases it.

The results for a shallow container system show that increasing modes exhibit decreasing aperiodic ranges, being true for both mode numbers m and n, and that decreasing liquid height ratio h/a increases the decay magnitude and decreases the oscillation frequency. Higher modes show stronger damping, and disappear fast as time goes on. The increase of the gravity parameter $g^* \equiv ga^3/v^2$ increases the aperiodic region, of which the increase is more pronounced for lower modes [29].

In what follows, an investigation of the coupled frequencies of the hydroelastic system consisting of a rigid circular tank of large aspect ratio h/a, filled with incompressible viscous liquid, the liquid surface of which is covered by an elastic element (membrane or thin plate). The lower portion of the liquid does not participate much in the motion of the liquid and behaves nearly like rigid body. This indicates that the velocity distribution at the bottom is quite small and assumes only very small values in radial- and angular direction. For that reason, it is considered vanishing in the following approximation theory. The large magnitude of the side wall velocities requires, however, to satisfy all boundary conditions there, yielding a much more involved complexity of the analysis.

2. Basic equations and solution

A circular cylindrical tank of diameter $2a$ (Fig. 1) is filled to a height $h>a$ with an incompressible and viscous liquid of density ρ and dynamic viscosity $\bar{\eta}$. The container side wall $r=a$ and the bottom of the tank $z=-h$ are rigid, while the free surface at $z=0$ is totally covered with a flexible membrane or an elastic plate. The plate may exhibit various attachments to the cylinder wall. It may be clamped, simply-supported, free, guided or it may be elastically supported. Assuming small displacements and velocities such that the motion of

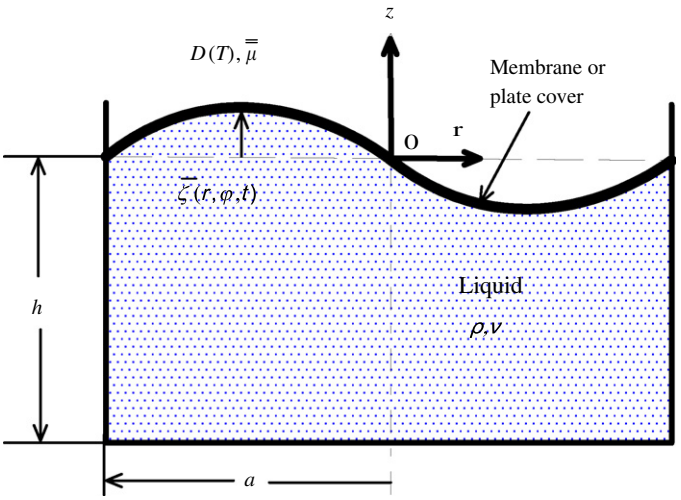

Fig. 1. Cylindrical container with an elastic cover filled with viscous liquid.

the liquid-structure system satisfies the Stokes equations

$$\frac{\partial u}{\partial t}+\frac{1}{\rho}\frac{\partial p}{\partial r}=\nu\left[\frac{\partial^2 u}{\partial r^2}+\frac{1}{r}\frac{\partial u}{\partial r}-\frac{u}{r^2}+\frac{1}{r^2}\frac{\partial^2 u}{\partial\varphi^2}+\frac{\partial^2 u}{\partial z^2}-\frac{2}{r^2}\frac{\partial \upsilon}{\partial\varphi}\right], \tag{1a}$$

$$\frac{\partial \upsilon}{\partial t}+\frac{1}{\rho}\frac{\partial p}{r\partial\varphi}=\nu\left[\frac{\partial^2 \upsilon}{\partial r^2}+\frac{1}{r}\frac{\partial \upsilon}{\partial r}-\frac{\upsilon}{r^2}+\frac{1}{r^2}\frac{\partial^2 \upsilon}{\partial\varphi^2}+\frac{\partial^2 \upsilon}{\partial z^2}+\frac{2}{r^2}\frac{\partial u}{\partial\varphi}\right], \tag{1b}$$

$$\frac{\partial w}{\partial t}+\frac{1}{\rho}\frac{\partial p}{\partial z}=\nu\left[\frac{\partial^2 w}{\partial r^2}+\frac{1}{r}\frac{\partial w}{\partial r}+\frac{1}{r^2}\frac{\partial^2 w}{\partial\varphi^2}+\frac{\partial^2 w}{\partial z^2}\right]-g, \tag{1c}$$

and the continuity equation

$$\frac{\partial u}{\partial r}+\frac{u}{r}+\frac{1}{r}\frac{\partial \upsilon}{\partial\varphi}+\frac{\partial w}{\partial z}=0, \tag{2}$$

where $\nu=\bar{\eta}/\rho$ is the kinematic viscosity, $\vec{v}=u\vec{e}_r+v\vec{e}_\varphi+w\vec{k}$ is the velocity and p the liquid pressure. These equations have to be solved simultaneously with the equation of the elastic cover, which in case of a flexible membrane is

$$T\left[\frac{\partial^2\bar{\zeta}}{\partial r^2}+\frac{1}{r}\frac{\partial\bar{\zeta}}{\partial r}+\frac{1}{r^2}\frac{\partial^2\bar{\zeta}}{\partial\varphi^2}\right]=\bar{\mu}\frac{\partial^2\bar{\zeta}}{\partial t^2}-\left(p-2\bar{\eta}\frac{\partial w}{\partial z}\right)_{z=0}, \tag{3a}$$

or in case of an elastic plate

$$\bar{D}\left[\frac{\partial^2}{\partial r^2}+\frac{1}{r}\frac{\partial}{\partial r}+\frac{1}{r^2}\frac{\partial^2}{\partial\varphi^2}\right]^2\bar{\zeta}+\bar{\mu}\frac{\partial^2\bar{\zeta}}{\partial t^2}=\left(p-2\bar{\eta}\frac{\partial w}{\partial z}\right)_{z=0}, \tag{3b}$$

and the appropriate boundary conditions. In these equations, T is the tension of the membrane, $\bar{\zeta}(r,\varphi,t)$ its deflection in z-direction, $\bar{\mu}$ the mass per unit area, $\bar{D}=E\bar{\delta}^3/12(1-\bar{\nu}^2)$ the flexural rigidity of the plate of thickness $\bar{\delta}$, $\bar{\nu}$ Poisson's ratio and E is Young's modulus of elasticity. The pressure distribution is given by

$$p(r,\varphi,z,t)=p_o-\rho gz+\bar{p}(r,\varphi,z,t).$$

Actually, the plate exhibits displacement ξ, η and $\bar{\zeta}$ in radial-, circumferential- and axial (normal) directions. This would require the coupled equations in ξ, η, and $\bar{\zeta}$ and in addition the compatibility conditions

$$\frac{\partial\xi}{\partial t}=u,\quad \frac{\partial\eta}{\partial t}=\upsilon\quad\text{and}\quad\frac{\partial\bar{\zeta}}{\partial t}=w,\quad\text{at } z=0.$$

Assuming, however, the radial- and circumferential deflections are small in comparison with the normal deflection $\bar{\zeta}(r,\varphi,t)$ results in the boundary conditions at the cover:

$$u = \upsilon = 0 \quad \text{and} \quad \frac{\partial\bar{\zeta}}{\partial t} = w, \quad \text{at } z = 0. \tag{4}$$

We assume u, υ, w and $\bar{p}$ are proportional to $e^{im\varphi}e^{st}$ (m integer, i.e. $u = e^{st}\sum_{m=0}^{\infty} U_m(r,z)e^{im\varphi}$, etc.), where $s = \bar{\sigma} + i\bar{\omega}$ is the complex frequency (coupled frequency of liquid and structure) to be determined. Then the Stokes equations (1) yield with

$$\phi = U_m + iV_m \quad \text{and} \quad \psi = U_m - iV_m, \tag{5a}$$

$$U_m = \frac{1}{2}(\phi + \psi) \quad \text{and} \quad V_m = \frac{i}{2}(\psi - \phi), \tag{5b}$$

the expressions

$$\frac{\partial^2\phi}{\partial r^2} + \frac{1}{r}\frac{\partial\phi}{\partial r} - \left[\frac{(m+1)^2}{r^2} + \frac{s}{v}\right]\phi + \frac{\partial^2\phi}{\partial z^2} = \frac{1}{\bar{\eta}}\left[\frac{\partial\overline{P}}{\partial r} - \frac{m}{r}\overline{P}\right], \tag{6a}$$

$$\frac{\partial^2\psi}{\partial r^2} + \frac{1}{r}\frac{\partial\psi}{\partial r} - \left[\frac{(m-1)^2}{r^2} + \frac{s}{v}\right]\psi + \frac{\partial^2\psi}{\partial z^2} = \frac{1}{\bar{\eta}}\left[\frac{\partial\overline{P}}{\partial r} + \frac{m}{r}\overline{P}\right], \tag{6b}$$

$$\frac{\partial^2 W}{\partial r^2} + \frac{1}{r}\frac{\partial W}{\partial r} - \left[\frac{m^2}{r^2} + \frac{s}{v}\right]W + \frac{\partial^2 W}{\partial z^2} = \frac{1}{\bar{\eta}}\frac{\partial\overline{P}}{\partial z}. \tag{6c}$$

Satisfying the normal boundary condition at the container bottom $z = -h$ with

$$\phi(r,z) = \Phi^*(r)\cosh[k(z+h)], \tag{7}$$

$$\psi(r,z) = \Psi^*(r)\cosh[k(z+h)], \tag{8}$$

$$W(r,z) = W^*(r)\sinh[k(z+h)], \tag{9}$$

$$\bar{P}(r,z) = P^*(r)\cosh[k(z+h)], \tag{10}$$

yields

$$\frac{d^2\Phi^*}{dr^2} + \frac{1}{r}\frac{d\Phi^*}{dr} - \left[\frac{(m+1)^2}{r^2} + \frac{s}{v} - k^2\right]\Phi^* = \frac{1}{\bar{\eta}}\left[\frac{dP^*}{dr} - \frac{m}{r}P^*\right], \tag{11a}$$

$$\frac{d^2\psi^*}{dr^2} + \frac{1}{r}\frac{d\psi^*}{dr} - \left[\frac{(m-1)^2}{r^2} + \frac{s}{v} - k^2\right]\psi^* = \frac{1}{\bar{\eta}}\left[\frac{dP^*}{dr} + \frac{m}{r}P^*\right], \tag{11b}$$

$$\frac{d^2 W^*}{dr^2} + \frac{1}{r}\frac{dW^*}{dr} - \left[\frac{m^2}{r^2} + \frac{s}{v} - k^2\right]W^* = \frac{k}{\bar{\eta}}P^*. \tag{11c}$$

The application of the vector operation "divergence" to the Stokes equations yields the Laplace equation for the pressure distribution, i.e.

$$\Delta\bar{p} = 0, \tag{12}$$

with the solution

$$\bar{p}(r,\varphi,z,t) = \sum_{m=0}^{\infty}\bar{D}_m J_m(kr)\cosh[k(z+h)]e^{im\varphi}e^{st}. \tag{13}$$

This renders for the right-hand sides of Eqs. (11a)–(11c), the expressions $-(k/\bar{\eta})\bar{D}_m J_{m+1}(kr)$, $(k/\bar{\eta})\bar{D}_m J_{m-1}(kr)$ and $(k/\bar{\eta})\bar{D}_m J_m(kr)$, respectively, while the continuity equation yields

$$\frac{d\Phi^*}{dr} + \frac{(m+1)}{r}\Phi^* + \frac{d\Psi^*}{dr} - \frac{(m-1)}{r}\Psi^* = -2kW^*. \tag{14}$$

The solution of the Eqs. (11a)–(11c) are given with $K \equiv ka$ and $S \equiv sa^2/v$ by

$$\Phi^*(r) = AJ_{m+1}\left(\sqrt{K_{mn}^2 - S}\,\frac{r}{a}\right) + D\frac{K_{mn}}{S}J_{m+1}\left(K_{mn}\frac{r}{a}\right), \tag{15a}$$

$$\Psi^*(r) = BJ_{m-1}\left(\sqrt{K_{mn}^2 - S}\,\frac{r}{a}\right) - D\frac{K_{mn}}{S}J_{m-1}\left(K_{mn}\frac{r}{a}\right), \tag{15b}$$

$$W^*(r) = CJ_m\left(\sqrt{K_{mn}^2 - S}\,\frac{r}{a}\right) - D\frac{K_{mn}}{S}J_m\left(K_{mn}\frac{r}{a}\right). \tag{15c}$$

From the continuity equation (14), we obtain

$$C = -\frac{\sqrt{K_{mn}^2 - S}}{2K_{mn}}(A - B). \tag{16}$$

With these results, the velocity- and pressure distribution may be expressed as ($\bar{D}_m(\bar{\eta}/a) \equiv D_m$)

$$u(r,\varphi,z,t) = \frac{1}{2}\,\mathrm{e}^{st}\sum_{m=0}^{\infty}\sum_{n=1}^{\infty}\left\{A_{mn}J_{m+1}\left(\sqrt{K_{mn}^2 - S}\frac{r}{a}\right) + B_{mn}J_{m-1}\left(\sqrt{K_{mn}^2 - S}\frac{r}{a}\right) - \frac{2K_{mn}}{S}D_{mn}J'_m\left(K_{mn}\frac{r}{a}\right)\right\} \times \cosh\left[K_{mn}\frac{(z+h)}{a}\right]\mathrm{e}^{\mathrm{i}m\varphi}, \tag{17}$$

$$v(r,\varphi,z,t) = -\frac{\mathrm{i}}{2}\,\mathrm{e}^{st}\sum_{m=0}^{\infty}\sum_{n=1}^{\infty}\left\{A_{mn}J_{m+1}\left(\sqrt{K_{mn}^2 - S}\frac{r}{a}\right) - B_{mn}J_{m-1}\left(\sqrt{K_{mn}^2 - S}\frac{r}{a}\right) + \frac{2m}{S(r/a)}D_{mn}J_m\left(K_{mn}\frac{r}{a}\right)\right\} \times \cosh\left[K_{mn}\frac{(z+h)}{a}\right]\mathrm{e}^{\mathrm{i}m\varphi}, \tag{18}$$

$$w(r,\varphi,z,t) = -\frac{1}{2}\,\mathrm{e}^{st}\sum_{m=0}^{\infty}\sum_{n=1}^{\infty}\left\{\frac{\sqrt{K_{mn}^2 - S}}{K_{mn}}(A_{mn} - B_{mn})J_m\left(\sqrt{K_{mn}^2 - S}\frac{r}{a}\right) + \frac{2K_{mn}}{S}D_{mn}J_m\left(K_{mn}\frac{r}{a}\right)\right\} \times \sinh\left[K_{mn}\frac{(z+h)}{a}\right]\mathrm{e}^{\mathrm{i}m\varphi}, \tag{19}$$

and

$$p(r,\varphi,z,t) = p_0 - \rho g z + \frac{\bar{\eta}\mathrm{e}^{st}}{a}\sum_{m=0}^{\infty}\sum_{n=1}^{\infty}D_{mn}J_m\left(K_{mn}\frac{r}{a}\right)\cosh\left[\frac{K_{mn}(z+h)}{a}\right]\mathrm{e}^{\mathrm{i}m\varphi}. \tag{20}$$

The boundary conditions that have to be satisfied are the side wall conditions (adhesive)

$$u = v = w = 0, \quad \text{at } r = a, \tag{21}$$

the tank bottom conditions

$$u = v = w = 0, \quad \text{at } z = -h, \tag{22}$$

of which only the normal condition $w = 0$ at $z = -h$ is already satisfied. The adhesive conditions $u = v = 0$ at the container bottom cannot be satisfied and are omitted for the above reason. They are, however, of minor influence if the liquid height ratio h/a is large (say $h/a > 1$), since the lower part of the liquid is acting nearly as a rigid body [32,33].

In addition to these boundary conditions at the rigid walls, we have to satisfy the condition at $z = 0$, the elastic cover condition (3) and the compatibility conditions (4). The boundary conditions (21) determine the

magnitude $K_{mn}(S)$ and yield for its determination the determinant

$$\begin{vmatrix} J_{m+1}\left(\sqrt{K_{mn}^2-S}\right) & J_{m-1}\left(\sqrt{K_{mn}^2-S}\right) & -2K_{mn}J'_m(K_{mn})/S \\ J_{m+1}\left(\sqrt{K_{mn}^2-S}\right) & -J_{m-1}\left(\sqrt{K_{mn}^2-S}\right) & 2mJ_m(K_{mn})/S \\ \sqrt{K_{mn}^2-S}J_m\left(\sqrt{K_{mn}^2-S}\right) & -\sqrt{K_{mn}^2-S}J_m\left(\sqrt{K_{mn}^2-S}\right) & 2K_{mn}^2J_m(K_{mn})/S \end{vmatrix} = 0. \tag{23}$$

For a fixed given angular mode m, the values $K_{mn}(S)$ must be obtained. From Eq. (21), we also obtain the magnitude of B_{mn} and D_{mn} as

$$B_{mn} = -\frac{J_{m+1}\left(\sqrt{K_{mn}^2-S}\right)J_{m-1}(K_{mn})}{J_{m-1}\left(\sqrt{K_{mn}^2-S}\right)J_{m+1}(K_{mn})}A_{mn} \equiv -\beta_{mn}A_{mn}, \tag{24}$$

and

$$D_{mn} = -\frac{SJ_{m+1}\left(\sqrt{K_{mn}^2-S}\right)}{K_{mn}J_{m+1}(K_{mn})}A_{mn} \equiv -S\gamma_{mn}A_{mn}. \tag{25}$$

From Eq. (4), we obtain, for $u = v = 0$ at $z = 0$ the expression (for fixed m)

$$\sum_{n=1}^{\infty} A_{mn}\left\{J_{m+1}\left(\sqrt{K_{mn}^2-S}\frac{r}{a}\right) - \beta_{mn}J_{m-1}\left(\sqrt{K_{mn}^2-S}\frac{r}{a}\right) + 2K_{mn}\gamma_{mn}J'_m\left(K_{mn}\frac{r}{a}\right)\right\}\cosh\left(K_{mn}\frac{h}{a}\right) = 0, \tag{26}$$

and

$$\sum_{n=1}^{\infty} A_{mn}\left\{J_{m+1}\left(\sqrt{K_{mn}^2-S}\frac{r}{a}\right) + \beta_{mn}J_{m-1}\left(\sqrt{K_{mn}^2-S}\frac{r}{a}\right) - \frac{2m}{(r/a)}\gamma_{mn}J_m\left(K_{mn}\frac{r}{a}\right)\right\}\cosh\left(K_{mn}\frac{h}{a}\right) = 0. \tag{27}$$

These equations are still functions of r/a and have to be satisfied at a finite number of points $r/a = \lambda/M$, where $\lambda = (0), 1, 2, \ldots, (M-1)$ (for $0 \leqslant r/a < 1$), i.e. we will employ the so-called collocation method. There are, however, the surface cover equations that have to be treated.

2.1. Membrane cover

If the liquid surface is covered by a flexible membrane, we have to solve Eq. (3a) with the boundary condition

$$\bar{\zeta} = 0, \quad \text{at } r = a. \tag{28}$$

This means with Eq. (4) ($\partial\bar{\zeta}/\partial t = w$) and

$$\bar{\zeta}(r,\varphi,t) = \sum_{m=0}^{\infty}\bar{\zeta}_m(r)e^{im\varphi}e^{st} = \sum_{m=0}^{\infty}\sum_{n=1}^{\infty}\left\{\bar{\xi}_{mn1}J_m\left(\sqrt{K_{mn}^2-S}\frac{r}{a}\right) + \bar{\xi}_{mn2}J_m\left(K_{mn}\frac{r}{a}\right)\right\}e^{im\varphi}e^{st}, \tag{29}$$

as well as Eq. (3a) that the equation

$$\frac{d^2\bar{\zeta}}{dr^2} + \frac{1}{r}\frac{d\bar{\zeta}_m}{dr} - \left(\frac{m^2}{r^2}+\frac{\beta^2}{a^2}\right)\bar{\zeta}_m = \frac{\bar{\eta}}{Ta}\sum_{n=1}^{\infty}\gamma_{mn}A_{mn}(S+2K_{mn}^2)J_m\left(K_{mn}\frac{r}{a}\right)\cosh\left(K_{mn}\frac{h}{a}\right) - \frac{\bar{\eta}}{Ta}\sum_{n=1}^{\infty}A_{mn}(1+\beta_{mn})\sqrt{K_{mn}^2-S}J_m\left(\sqrt{K_{mn}^2-S}\frac{r}{a}\right)\cosh\left(K_{mn}\frac{h}{a}\right), \tag{30}$$

where $\beta^2 \equiv a^2(\bar{\mu}s^2 + \rho g)/T$, has to be solved. The solution of the above inhomogeneous differential equation yields the expression

$$\bar{\zeta}_m(r) = A_{om} I_m\left(\beta \frac{r}{a}\right) - \frac{\bar{\eta} a}{T} \sum_{n=1}^{\infty} A_{mn} \gamma_{mn} \frac{\left(S + 2K_{mn}^2\right) \cosh\left(K_{mn}(h/a)\right)}{\left(K_{mn}^2 + \beta^2\right)} J_m\left(K_{mn} \frac{r}{a}\right)$$
$$+ \frac{\bar{\eta} a}{T} \sum_{n=1}^{\infty} A_{mn}\left(1 + \beta_{mn}\right) \frac{\sqrt{K_{mn}^2 - S} \cosh\left(K_{mn}(h/a)\right)}{\left(K_{mn}^2 - S + \beta^2\right)} J_m\left(\sqrt{K_{mn}^2 - S} \frac{r}{a}\right). \tag{31}$$

Introducing $A_{mn} a^2/\nu = A_{mn}^*$ and $Ta/(\rho \nu^2) \equiv T^*$, we obtain

$$\bar{\zeta}_m(r) = A_{om} I_m\left(\beta \frac{r}{a}\right) - \frac{1}{T^*} \sum_{n=1}^{\infty} A_{mn}^* \gamma_{mn} \frac{\left(S + 2K_{mn}^2\right) \cosh\left(K_{mn}(h/a)\right)}{\left(K_{mn}^2 + \beta^2\right)} J_m\left(K_{mn} \frac{r}{a}\right)$$
$$+ \frac{1}{T^*} \sum_{n=1}^{\infty} A_{mn}^*\left(1 + \beta_{mn}\right) \frac{\sqrt{K_{mn}^2 - S} \cosh\left(K_{mn}(h/a)\right)}{\left(K_{mn}^2 - S + \beta^2\right)} J_m\left(\sqrt{K_{mn}^2 - S} \frac{r}{a}\right). \tag{32}$$

Since the membrane is clamped at $r = a$, it is

$$\bar{\zeta}_m(a) = A_{om} I_m(\beta) + \frac{1}{T^*} \sum_{n=1}^{\infty} A_{mn}^* \left\{ \left(1 + \beta_{mn}\right) \frac{\sqrt{K_{mn}^2 - S}}{\left(K_{mn}^2 - S + \beta^2\right)} J_m\left(\sqrt{K_{mn}^2 - S}\right) - \frac{\gamma_{mn}\left(S + 2K_{mn}^2\right)}{\left(K_{mn}^2 + \beta^2\right)} J_m(K_{mn}) \right\}$$
$$\times \cosh\left(K_{mn} \frac{h}{a}\right) = 0. \tag{33}$$

With the compatibility condition (4), i.e. $\partial \bar{\zeta}/\partial t = w$ at $z = 0$, we obtain

$$\bar{\xi}_{mn1} = -\frac{\sqrt{K_{mn}^2 - S}}{2SK_{mn}} A_{mn}^*\left(1 + \beta_{mn}\right) \sinh\left(K_{mn} \frac{h}{a}\right),$$

and

$$\bar{\xi}_{mn2} = \frac{K_{mn}}{S} \gamma_{mn} A_{mn}^* \sinh\left(K_{mn} \frac{h}{a}\right).$$

It is therefore by comparison of the results with Eq. (32)

$$A_{om} I_m\left(\beta \frac{r}{a}\right) + \frac{1}{T^*} \sum_{n=1}^{\infty} A_{mn}^* \left\{ \left(1 + \beta_{mn}\right) \frac{\sqrt{K_{mn}^2 - S}}{\left(K_{mn}^2 - S + \beta^2\right)} J_m\left(\sqrt{K_{mn}^2 - S} \frac{r}{a}\right) - \frac{\gamma_{mn}\left(S + 2K_{mn}^2\right)}{\left(K_{mn}^2 + \beta^2\right)} J_m\left(K_{mn} \frac{r}{a}\right) \right\}$$
$$\times \cosh\left(K_{mn} \frac{h}{a}\right) + \sum_{n=1}^{\infty} A_{mn}^* \left\{ \left(1 + \beta_{mn}\right) \frac{\sqrt{K_{mn}^2 - S}}{2SK_{mn}} J_m\left(\sqrt{K_{mn}^2 - S} \frac{r}{a}\right) - \frac{K_{mn}}{S} \gamma_{mn} J_m\left(K_{mn} \frac{r}{a}\right) \right\}$$
$$\times \sinh\left(K_{mn} \frac{h}{a}\right) = 0. \tag{34}$$

We shall satisfy the Eqs. (26), (27) and (34), which are equations in A_{mn}^* at M points $r/a = \lambda/M$, $\lambda = 0, 1, 2, \ldots, (M-1)$. This yields

$$\sum_{n=1}^{3M} A_{mn}^* \left\{ J_{m+1}\left(\sqrt{K_{mn}^2 - S} \frac{\lambda}{M}\right) - \beta_{mn} J_{m-1}\left(\sqrt{K_{mn}^2 - S} \frac{\lambda}{M}\right) + 2K_{mn} \gamma_{mn} J'_m\left(K_{mn} \frac{\lambda}{M}\right) \right\}$$
$$\times \cosh\left(K_{mn} \frac{h}{a}\right) = 0, \tag{35}$$

for $\lambda = (0), 1, 2, \ldots, (M-1)$,

$$\sum_{n=1}^{3M} A_{mn}^{*}\left\{J_{m+1}\left(\sqrt{K_{mn}^{2}-S}\,\frac{\lambda}{M}\right)+\beta_{mn}J_{m-1}\left(\sqrt{K_{mn}^{2}-S}\,\frac{\lambda}{M}\right)-\frac{2m\gamma_{mn}}{\lambda/M}J_{m}\left(K_{mn}\frac{\lambda}{M}\right)\right\} \times \cosh\left(K_{mn}\frac{h}{a}\right)=0, \tag{36}$$

for $\lambda = 1, 2, \ldots, (M-1)$. In addition, Eq. (34) results in

$$A_{om}I_{m}\left(\beta\frac{\lambda}{M}\right)+\sum_{n=1}^{3M}A_{mn}^{*}\left\{\frac{(1+\beta_{mn})\sqrt{K_{mn}^{2}-S}}{T^{*}\left(K_{mn}^{2}-S+\beta^{2}\right)}J_{m}\left(\sqrt{K_{mn}^{2}-S}\,\frac{\lambda}{M}\right)-\frac{\gamma_{mn}\left(S+2K_{mn}^{2}\right)}{T^{*}\left(K_{mn}^{2}+\beta^{2}\right)}J_{m}\left(K_{mn}\frac{\lambda}{M}\right)\right\} \times \cosh\left(K_{mn}\frac{h}{a}\right)+\sum_{n=1}^{3M}A_{mn}^{*}\left\{(1+\beta_{mn})\frac{\sqrt{K_{mn}^{2}-S}}{2SK_{mn}}J_{m}\left(\sqrt{K_{mn}^{2}-S}\,\frac{\lambda}{M}\right)-\frac{K_{mn}}{S}\gamma_{mn}J_{m}\left(K_{mn}\frac{\lambda}{M}\right)\right\} \times \sinh\left(K_{mn}\frac{h}{a}\right)=0, \tag{37}$$

for $\lambda = 1, 2, \ldots, M$, in which A_{0m} is obtained from Eq. (33). These are fully $3M-2$ (or $3M-1$) homogeneous algebraic equations in A_{mn}^{*} (m fixed, $n = 1, 2, \ldots, 3M-2$ (or $3M-1$)), of which the vanishing of the coefficient determinant represents the natural damped frequency equation for the determination of the approximate lower coupled complex natural frequencies. It may be noticed that these equations have to be solved together with the values $K_{mn}(S)$ from Eq. (23).

2.2. Plate cases

Plate cases may be treated in a similar way under the following boundary conditions, but are omitted here.

(a) clamped:

$$\zeta = 0 \quad \text{and} \quad \frac{\partial\zeta}{\partial r}=0, \quad \text{at } r=a, \tag{38}$$

(b) simply supported:

$$\zeta = 0,\ M_{r} = -\bar{D}\left[\frac{\partial^{2}\zeta}{\partial r^{2}}+\bar{\nu}\left(\frac{1}{r}\frac{\partial\zeta}{\partial r}+\frac{1}{r^{2}}\frac{\partial^{2}\zeta}{\partial\varphi^{2}}\right)\right]=0, \quad \text{at } r=a, \tag{39}$$

(c) free:

$$M_{r}=0 \quad \text{and} \quad V_{r}=-\bar{D}\frac{\partial}{\partial r}\left\{\frac{\partial^{2}\zeta}{\partial r^{2}}+\frac{1}{r}\frac{\partial\zeta}{\partial r}+\frac{1}{r^{2}}\frac{\partial^{2}\zeta}{\partial\varphi^{2}}\right\}-\frac{\bar{D}}{r}(1-\bar{\nu})\frac{\partial}{\partial r}\left(\frac{1}{r}\frac{\partial^{2}\zeta}{\partial\varphi^{2}}\right)=0, \quad \text{at } r=a, \tag{40}$$

(d) guided:

$$\frac{\partial\zeta}{\partial r}=0 \quad \text{and} \quad V_{r}=0, \quad \text{at } r=a, \tag{41}$$

(e) elastically supported:

$$M_{r}=\bar{K}\frac{\partial\zeta}{\partial r} \quad \text{and} \quad V_{r}=0, \quad \text{at } r=a, \tag{42}$$

where $\bar{\nu}$ and $\bar{D}$ are Poisson's ratio and flexural rigidity of the plate, respectively. The edge rotation is opposed by torsional springs having a distributed stiffness $\bar{K}$ (moment per unit length).

3. Numerical evaluations

Some of the above-obtained analytical results have been evaluated numerically and are presented here. The numerical evaluations have been restricted to a membrane cover (Fig. 1) for asymmetric motions, since this motion exhibits the lowest and most dangerous natural liquid frequency, which should be increased by an additional membrane cover. This shall yield a larger frequency and move it above and away from the control frequency. For a cover consisting of a flexible membrane, the characteristic parameters are the tension parameter $T^* \equiv Ta/\rho\nu^2$, the gravitational parameter $g^* \equiv ga^3/\nu^2$, the density ratio $\mu^* \equiv \bar{\mu}/\rho a$, the liquid height ratio h/a and the vibration modes (m, n), where m is the number of nodal diameters and n is the number of nodal circles (see Fig. 2). In the numerical computations, the number of unknown constants A_{mn} was taken to be 20. This yields reliable engineering data for the lower modes. The given results are especially of importance for large liquid height ratios h/a, for which the liquid in the lower part of the container behaves like a rigid body. For such liquid fillings, the motion of the liquid takes place immediately below the membrane, penetrating with its motion only to a depth of about one wave length. For this reason, the contribution to damping and frequency of the lower part of the liquid immediately above the tank bottom is of minor and negligible effect.

In previous investigations [32–34] of viscous liquid motion with free surface in a rigid cylindrical container, an important fact was detected. The results show that, for small liquid heights h/a, the liquid motion exhibits only an aperiodic motion, if disturbed. The decrease of the liquid surface tension $\sigma^* \equiv \sigma a/\rho\nu^2$, i.e. increase of viscosity ν, increases the region of aperiodicity and decreases the decay magnitude and oscillation frequency for h/a values above the aperiodic range. In addition, the aperiodic range decreases with increase of the gravitational parameter $g^* \equiv ga^3/\nu^2$. In the oscillation region, the frequency increases and the decay exhibits larger magnitude.

In the present numerical evaluations, the tension parameter was chosen to be $T^* = 1000$, while the gravitational parameter $g^* = 10\,000$ and the mass parameter $\mu^* = 0.01$.

In the following figures, we represent for these parameters the coupled frequency $\omega \equiv \bar{\omega}a^2/\nu = \mathrm{Im}(S)$ and $\delta = \bar{\sigma}a^2/\nu = \mathrm{Re}(S)$, both as functions of the liquid height ratio $0.8 \leqslant h/a \leqslant 2.0$. The results are again compared with previous results of the frictionless case and the viscous case for shallow liquid height, in which only the normal side wall condition has been satisfied, but all the bottom conditions (adhesive boundary conditions) have been observed [29].

In Fig. 3, we represent for $T^* = 1000$, $g^* = 10\,000$, $\mu^* = 0.01$ for the mode $m = 1$, $n = 1$, the results of the oscillation frequency ω and the decay magnitude δ of the motion. It may be mentioned that these results are valid for the here treated case of about $0.5 \leqslant h/a \leqslant 1.0$. The oscillation frequency $\dot{u}$ increases with increasing h/a and reaches soon a magnitude of about $\omega = 201$, while the decay magnitude δ approaches a value of about

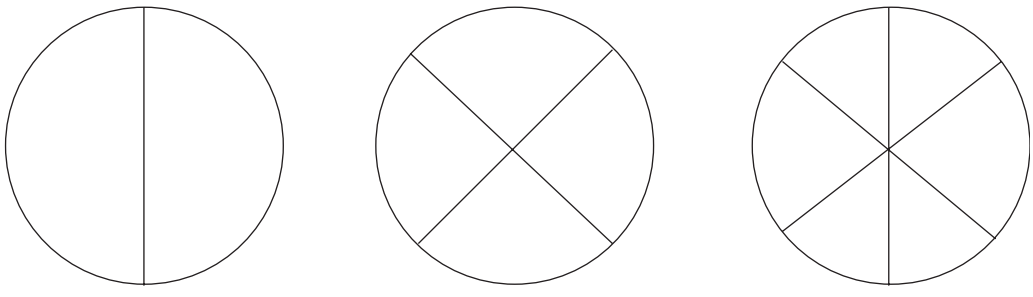

Fig. 2. Vibration modes of covered surface; $m = 1, 2, 3$.

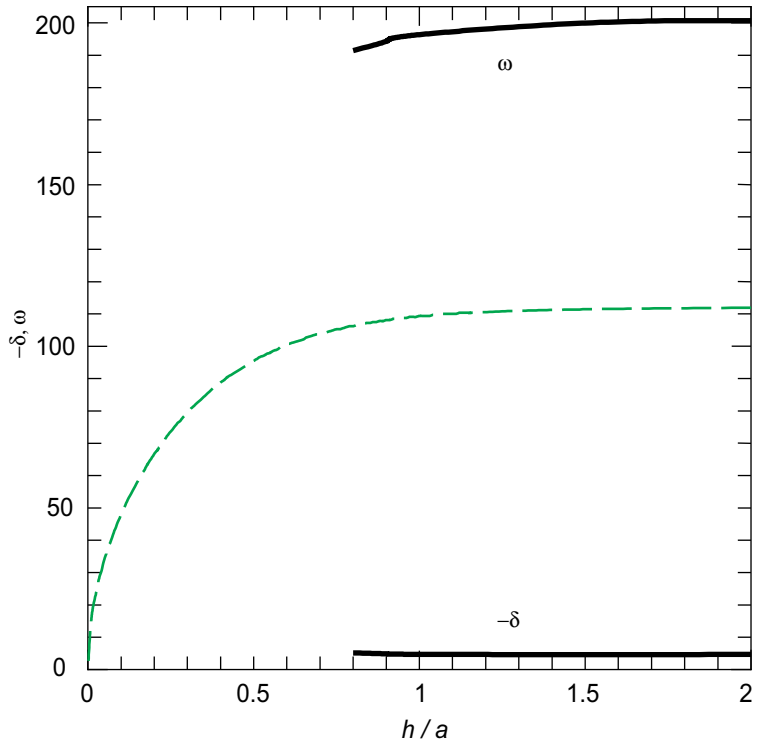

Fig. 3. Coupled complex frequency of asymmetric motion $m=1$, $n=1$; $T^*=10^3$, $g^*=10^4$ and $\mu^*=10^{-2}$; — — —, inviscid.

$\delta=-4.7$. In comparison, the dashed line represents the result for the coupled frequency of the lowest asymmetric mode $m=n=1$ for frictionless liquid, which also increases with increasing liquid height ratio, but assumes a much lower oscillation frequency. It should be mentioned here, that the shown mode $m=1$, $n=1$ represents the dynamically most important mode, since it exhibits the largest sloshing mass participating in the motion of the liquid-structure system and the lowest frequency of the system. Higher modes, i.e. $(m,n)=(1,2)$, $(1,3)$, $(2,1)$, $(2,2)$, $(2,3)$ or $(m,n)=(3,1)$, $(3,2)$, $(3,3)$, etc. exhibit rapidly decreasing participating slosh masses and higher frequencies, and may actually be neglected. They also will exhibit much larger decay magnitudes, expressing a rapid decay of the motion. As time goes on they will disappear in the liquid motion. Increasing the tension parameter T^* yields increasing oscillation frequencies $\dot{u}$ and also increased decay magnitude $|\delta|$. This means that large tension parameters will make the oscillations disappear much faster (not shown). The liquid in the shallow container shows in the mode $m=n=1$ only aperiodic motion, i.e. $\mathrm{Re}\,S\neq 0$. The decay magnitude is very large, is as shown in Ref. [29] (Fig. 10) beyond the treated $0<h/a<0.5$ range and cannot be presented in this Fig. 3. Due to the largest slosh mass ("slosh-plug"), the here treated case may only be valid for $0.8<h/a$. In Fig. 4, we present the results of the mode $m=1$, $n=2$ and notice, for a much larger oscillation frequency and much larger decay magnitude, the same behavior as in the previous mode. The oscillation frequency is about $3\frac{1}{2}$ times as large, while the decay $|\delta|$ assumes a magnitude of about $4\frac{1}{2}$ times that of the mode $m=n=1$. Fig. 5 shows oscillation frequency and decay magnitude for the mode $m=2$, $n=1$. In this case, the membrane exhibits two nodal lines, as may be seen in Fig. 2. The oscillation frequency reaches soon a value of $\omega=298$ and the decay magnitude $\delta=-13.5$, while the inviscid case exhibits an oscillation frequency of about $\dot{u}=239$. We notice that the difference of the oscillation frequency $\dot{u}$ for viscous liquid and that of inviscid liquid decreases as the angular modal number m assumes larger values. The validity of the coupled viscous results has been, due to the reduced sloshing mass, i.e. a lesser depth at which the "slosh-plug" below the membrane appears, increased. We assume that the presented results are valid in the range $0.5\leqslant h/a\leqslant 2.0$ (Fig. 5).

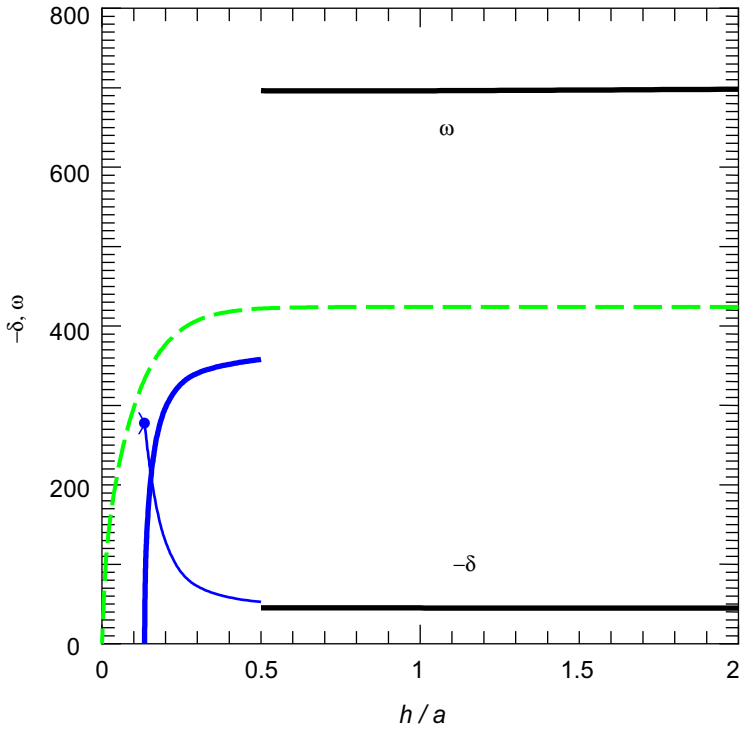

Fig. 4. Coupled complex frequency of asymmetric motion $m = 1$, $n = 2$; $T^* = 10^3$, $g^* = 10^4$ and $\mu^* = 10^{-2}$; — — —, inviscid, ——— and ———, viscous [29].

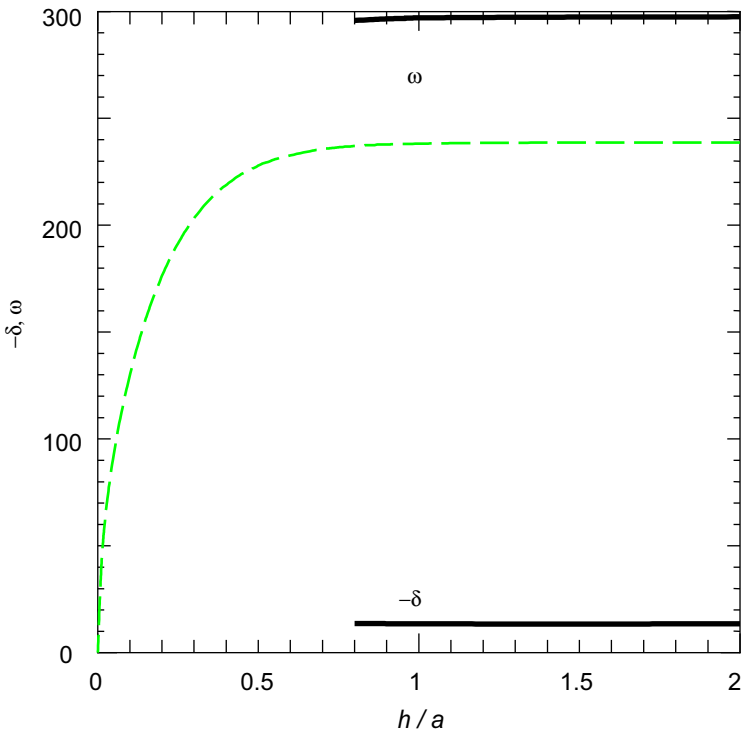

Fig. 5. Coupled complex frequency for asymmetric motion $m = 2$, $n = 1$; $T^* = 10^3$, $g^* = 10^4$ and $\mu^* = 10^{-2}$; — — —, inviscid.

From Fig. 10 of Ref. [29] we notice again that for $T^* = 10^3$ the system represents an aperiodic motion if disturbed in that mode $m = 2$, $n = 1$. The value $\mathrm{Re}\, S \neq 0$ cannot be given here, since Ref. [29] does not show the actual value. Similar results are shown for the third mode $m = 3$, $n = 1$ in Fig. 6. The results for viscous liquid reaches for liquid height ratios larger $h/a > 0.5$ a nearly constant magnitude of $\omega = 422$, while the decay magnitude exhibits in this area a value of about $\delta = -43.5$. This is, because the upper liquid participates from a certain liquid height on totally in the sloshing motion, and penetrates with increasing mode number less deep below the membrane into the liquid. The liquid motion exhibits three nodal lines (see Fig. 2) and shows that the oscillation frequency of the frictionless coupled frequency is much closer below the viscous case. For the mode $m = 3$, $n = 1$, the range of validity for the coupled viscous liquid-membrane results may, due to the very small slosh-plug mass immediately below the membrane, be further extended to about $0.3 \leqslant h/a \leqslant 2.0$. From Fig. 10 of Ref. [29], we find that the system for a shallow container yields for $0 \leqslant h/a \leqslant 0.16$ only the possibility of aperiodic motion. This is indicated by the thin blue line, reaching at $|\delta| \approx 200$ a bifurcation point at $h/a = 0.16$. Comparing the four, Figs. 3–6, we notice that for $m = 1, 2, 3$ and $n = 1$ the damping is significantly increasing with increasing mode number, i.e. from $|\delta| = 4.7$ for $m = 1$ to 43.5 for $m = 3$. This indicates that higher modes are due to their fast disappearance of minor importance. In addition, we detect that the oscillation frequency of the frictionless cases are quite different from those of the viscous cases, and that the difference of frictionless frequency and viscous oscillation frequency reduces as the mode number increases. This indicates that for higher modes the natural frequency is lower, but close to the oscillation frequency of the viscous case (see Table 1). This suggests that for higher modes, the frictionless treatment of the hydroelastic problem may yield good approximate results.

For higher modes, we noticed that the number of A_{mn} needs to be increased to obtain better results. This, however, has been omitted here, since we are mainly concerned with the lower modes for reasons of controlling the stability and response of a space vehicle. The axisymmetric case is presented in Ref. [35].

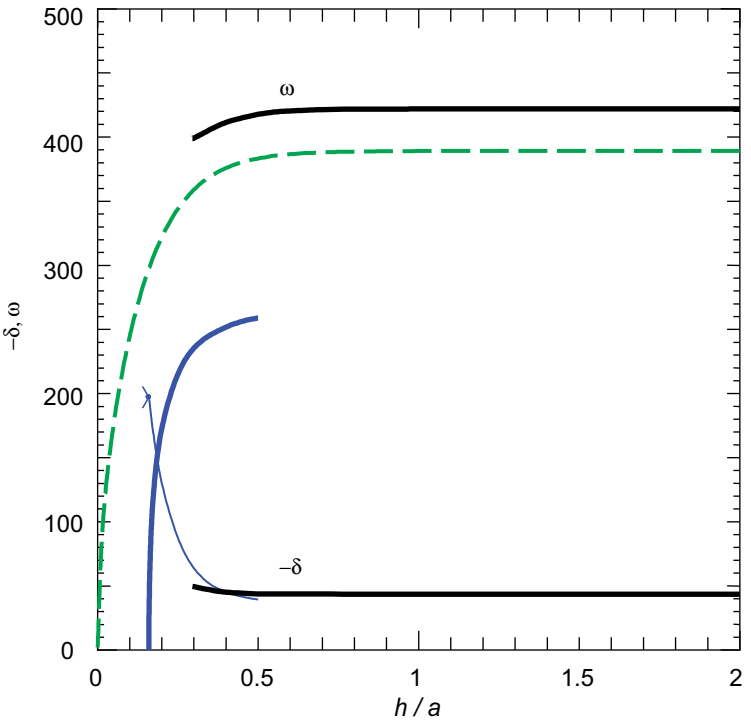

Fig. 6. Coupled complex frequency for asymmetric motion $m = 3$, $n = 1$; $T^* = 10^3$, $g^* = 10^4$ and $\mu^* = 10^{-2}$; – – – –, inviscid, ——— and ———, viscous [29].

Table 1
Coupled oscillation frequencies and decay magnitudes at $h/a = 2.0$

m	S_{m1}		S_{m2}	
	Frictionless	Viscous	Frictionless	Viscous
1	112i	$-4.7+201$i	424	$-44.9+698$i
2	239i	$-13.5+298$i	—	—
3	389i	$-43.5+422$i	—	—

4. Conclusion

From the above results, we may conclude some basic behavior of the liquid-structure system, using a membrane as a covering element of the free liquid surface for large aspect ratio systems.

1. With increasing liquid height ratio h/a, the coupled frequencies increase and reach soon a nearly constant value. This increase is stronger for higher modes (both angular and radial) where the frequency reaches a nearly constant magnitude at lower h/a values.
2. The decay magnitude decreases slightly with increasing liquid height ratio h/a and reaches soon nearly constant magnitude. For higher modes, a constant but larger magnitude is achieved at lower liquid height ratios. It also means that higher modes are damped out fast.
3. The coupled oscillation frequencies are always larger than those of a system of frictionless liquid, the differences of which become smaller with increasing mode numbers.

Acknowledgments

The authors would like to thank Dr. W. Eidel, Institut für Raumfahrttechnik, Universität der Bundeswehr München, for his helpful suggestions in the numerical method.

Appendix A

In the frictionless analysis [25], we employed the boundary conditions as, $u = \partial\phi/\partial r = 0$ at $r = a$ (at the wall), $\dot{\zeta} = w = \partial\phi/\partial z$ at $z = 0$ (at the liquid-membrane interface), and $w = \partial\phi/\partial z = 0$ at $z = -h$ (at the bottom). The validity of this solution, as has been mentioned already above, is only guaranteed for small h/a values, i.e. shallow containers. As h/a decreases in the shallow region ($h/a < 0.5$), the oscillation frequency decreases considerably, while the decay magnitude $|\delta|$ increases rapidly. The lower the liquid height ratio h/a becomes, the more of the total liquid volume (“slosh-plug”) (Fig. A1) participates in the liquid motion, thus increasing the decay magnitude even more. At a certain height h/a, the liquid-structure system ceases to oscillate and is just performing an aperiodic motion, if disturbed. This motion persists with decreasing liquid height ratio h/a and exhibits increasing decay magnitude $|\delta|$. We may notice [29] that with increasing angular mode m and increasing radial mode n the aperiodic range is decreasing. In addition we may remark that the oscillation frequency reaches at $h/a = 0.5$ a certain magnitude which for larger h/a-values still would increase slowly. This region, however, has not been investigated in Ref. [29]. The analytical approaches of shallow and large aspect ratio containers cannot, due to the different analytical procedures yield an acceptable transition region h/a. For the here treated case we may notice that with increasing liquid height ratio h/a, the coupled frequency increases, reaching soon a magnitude, for which only very little change occurs, as h/a increases beyond the region $h/a = 0.5$. The same is true for the decay behavior. For frictionless liquid, the frequency increases strongly for growing at small h/a-values and reaches also soon a value of nearly constant magnitude. Its magnitude is below that of the viscous liquid, as indicated by the dashed line (see Ref. [29]).

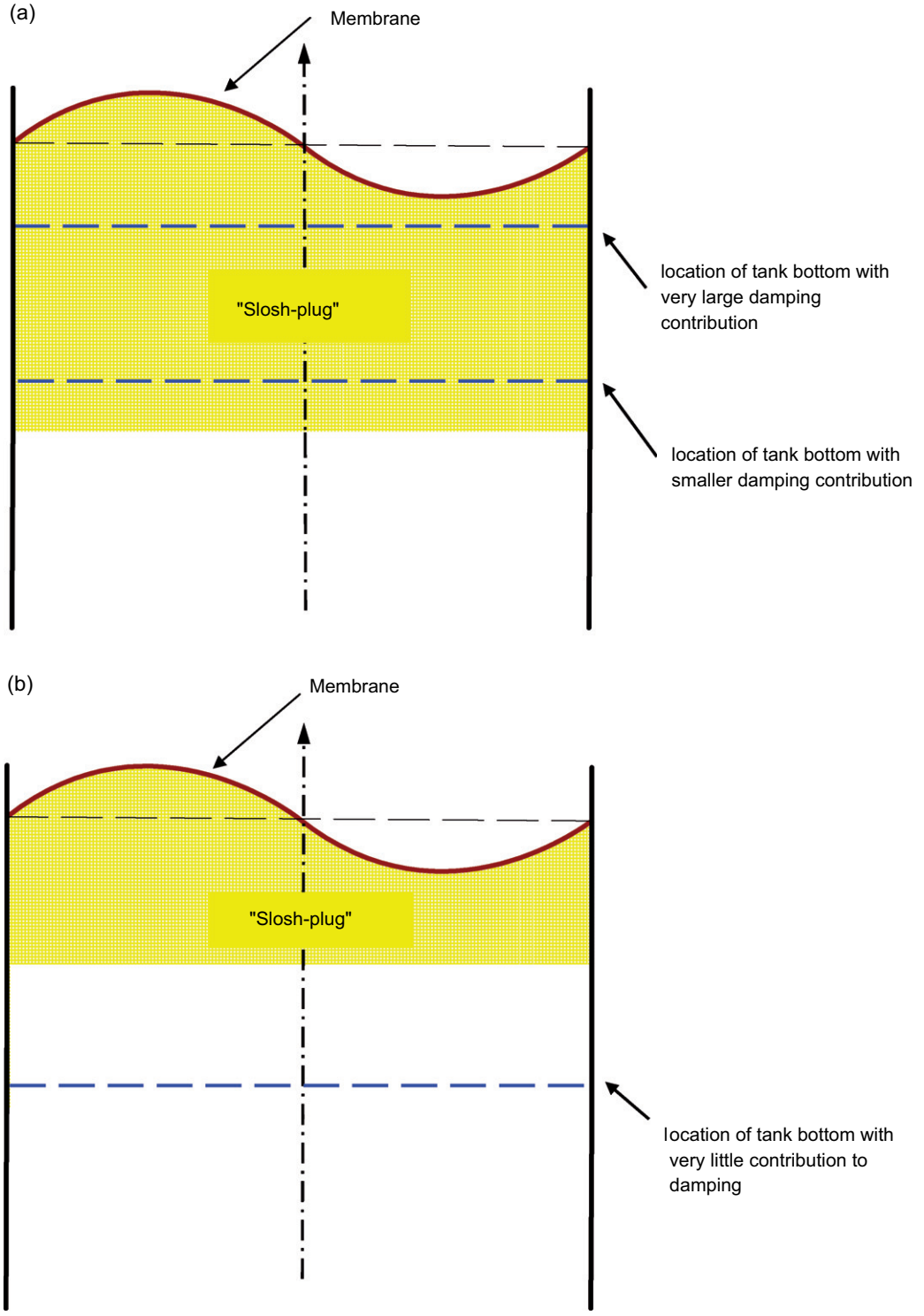

Fig. A1. "Slosh-plug" for various container bottom locations — — — and modes: (a) $m = n = 1$ mode, and (b) $m = 3$, $n = 1$ mode.

For a shallow container we notice: The strong damping as contributed from the top and bottom of the container reduces the oscillation frequency considerably, yielding for small aspect ratios even vanishing oscillation frequency and exhibits only an aperiodic motion of the liquid-membrane system. With increasing small h/a-values, the contribution of the bottom of the container to damping decreases due to the smaller velocity distribution in the growing "slosh-plug". It shall not suppress the growth of the oscillation frequency as much as that of a smaller (shallower) aspect ratio tank. With increasing location h/a of the container bottom, the liquid motion near the tank bottom becomes weaker, thus contributing less damping to the total liquid-structure system. If the bottom of the tank is located in the "slosh-plug", then it will contribute—due to larger velocity distribution—more damping to the system, thus reducing the oscillation frequency (see Fig. A1).

References

[1] H.F. Bauer, Flüssigkeitsschwingungen in Raketenbehältern und ihr Einfluss auf die Gesamtstabilität, *Zeitschrift für Flugwissenschaften* 12 (1964) Teil I 85–101, Teil II 222–229.
[2] H.F. Bauer, Liquid oscillations in a circular cylindrical container with "sliding" contact line, *Forschung im Ingenieurwesen* 58 (1992) 240–251.
[3] J.W. Miles, On the sloshing of liquid in a flexible tank, *Journal of Applied Mechanics E* 25 (1958) 277–283.
[4] U.S. Lindholm, D.D. Kana, H.N. Abramson, Breathing vibrations of a circular cylindrical shell with an internal liquid, *Journal of Aerospace Sciences* 29 (1962) 1052–1059.
[5] M.L. Baron, R. Skalak, Free vibrations of fluid-filled cylindrical shells, *Proceedings of the American Society of Civil Engineers* 88 (1962) 17–43.
[6] W.-H. Chu, Breathing vibrations of a partially filled cylinder tank-linear theory, *Journal of Applied Mechanics E* 30 (1963) 532–536.
[7] E. Saleme, T. Liber, Breathing vibrations of pressurized partially filled tanks, *Journal of the American Institute of Aeronautics and Astronautics* 3 (1965) 132–136.
[8] T.Y. Tsui, N.C. Small, Hydroelastic oscillations of a liquid surface in an annular circular cylindrical tank with flexible bottom, *Journal of Spacecraft and Rockets* 5 (1968) 202–206.
[9] P.G. Bhuta, G. Pravin, L.R. Koval, Coupled oscillations of a liquid with a free surface in a tank, *Zeitschrift für Angewandte Mathematik und Physik* 15 (1964) 466–480.
[10] P.G. Bhuta, L.R. Koval, Hydroelastic solution of the sloshing of a liquid in a cylindrical tank, *Journal of the Acoustical Society of America* 36 (1964) 2071–2079.
[11] N. Yamaki, J. Tani, T. Yamaji, Free vibration of a clamped–clamped circular cylindrical shell partially filled with liquid, *Journal of Sound and Vibration* 94 (1984) 531–550.
[12] H.F. Bauer, T.M. Hsu, J.T.S. Wang, Interaction of a sloshing liquid with elastic containers, *Transactions of ASME, Journal of Basic Engineering* 90 (1968) 373–377.
[13] H.F. Bauer, J. Siekmann, J.T.S. Wang, Axisymmetric hydroelastic sloshing in an annular cylindrical container, *Journal of Spacecraft and Rockets* 5 (1968) 981–983.
[14] H.F. Bauer, J.T.S. Wang, P.Y. Chen, Axisymmetric hydroelastic sloshing in a circular cylindrical container, *Aeronautical Journal* 76 (1972) 704–712.
[15] H.F. Bauer, J. Siekmann, Note on linear hydroelastic sloshing, *Zeitschrift für Angewandte Mathematik und Mechanik* 49 (1969) 577–589.
[16] H.F. Bauer, J. Siekmann, Dynamic interaction of a liquid with the elastic structure of a circular cylindrical container, *Ingenieur Archiv* 40 (1971) 266–280.
[17] H.F. Bauer, Hydroelastische Schwingungen im aufrechten Kreiszylinderbehälter, *Zeitschrift für Flugwissenschaften* 18 (1970) 117–134.
[18] H.F. Bauer, Hydroelastische Schwingungen in einem starren Kreiszylinder bei elastischer Flüssigkeitsoberflächenabdeckung, *Zeitschift für Flugwissenschaften* 21 (1973) 202–213.
[19] A.A. Lakis, M.P. Paidoussis, Free vibration of cylindrical shells partially filled with liquid, *Journal of Sound and Vibration* 19 (1971) 1–15.
[20] W.E. Stillman, Free vibration of cylinders containing liquid, *Journal of Sound and Vibration* 30 (1973) 509–524.
[21] R.K. Jain, Vibration of fluid-filled, orthotropic cylindrical shells, *Journal of Sound and Vibration* 37 (1974) 379–388.
[22] W.A Nash, S.H. Shaaban, T Monzakis, Response of liquid storage tanks to seismic motion, *Proceedings of the Third IUTAM Symposium on Shell Theory*, North-Holland, Amsterdam, 1980, pp. 393–403.
[23] M.A. Haroun, G.W. Housner, Earthquake response of deferrable liquid storage tanks, *Journal of Applied Mechanics E* 48 (1981) 411–418.
[24] T. Balendra, K.K.P. Paramasivam, S.L. Lee, Free vibration analysis of cylindrical liquid storage tanks, *International Journal of Mechanical Science* 24 (1982) 47–59.
[25] H.F. Bauer, Coupled frequencies of a liquid in a circular cylindrical container with elastic liquid surface cover, *Journal of Sound and Vibrations* 180 (1995) 689–704.

[26] H.F. Bauer, Hydroelastic vibrations in a rectangular container, *International Journal of Solids and Structures* 17 (1981) 639–652.
[27] H.F. Bauer, W. Eidel, Hydroelastic vibrations in a rectangular container filled with frictionless liquid and partly elastically covered free surface, *Journal of Fluids and Structures* 19 (2004) 209–220.
[28] H.F. Bauer, K. Komatsu, Coupled frequencies of a frictionless liquid in a circular cylindrical tank with an elastic partial surface cover, *Journal of Sound and Vibration* 230 (2000) 1147–1163.
[29] H.F. Bauer, M. Chiba, Hydroelastic viscous oscillations in a circular cylindrical container with an elastic cover, *Journal of Fluids and Structures* 14 (2000) 917–936.
[30] H.F. Bauer, W. Eidel, Free oscillations and response of a viscous liquid in a rigid circular cylindrical tank, *Aerospace Science and Technology* 3 (1999) 495–512.
[31] H.F. Bauer, W. Eidel, Analytical determination of interior and boundary layer damping of sloshing waves in a circular cylinder, Universität der Bundeswehr München, Germany, Forschungsbericht LRT-WE-9-FB-2, 2001.
[32] H.F. Bauer, W. Eidel, Axisymmetric viscous liquid oscillations in a cylindrical container, *Forschung im Ingenieurwesen* 63 (1997) 189–201.
[33] H.F. Bauer, W. Eidel, Oscillations of a viscous liquid in a cylindrical container, *Aerospace Science and Technology* 8 (1997) 519–532.
[34] H.F. Bauer, W. Eidel, Axisymmetric natural damped frequencies of a viscous liquid in a circular cylindrical container—An alternative semi-analytical solution, *Forschung im Ingenieurwesen* 65 (1999) 191–199.
[35] H.F. Bauer, M. Chiba, Axisymmetric oscillation of a viscous liquid covered by an elastic structure, *Journal of Sound and Vibration* 281 (2005) 835–847.